A novel prokaryotic CRISPR-Cas12a based tool for programmable transcriptional activation and repression

Christoph Schilling[1], Mattheos Koffas[2,3], Volker Sieber[1,4,5,6] and Jochen Schmid[1,7]

1) Chair of Chemistry of Biogenic Resources, Technical University of Munich, Campus for Biotechnology and Sustainability, Schulgasse 16, 94315, Straubing, Germany
2) Center for Biotechnology and Interdisciplinary Studies, Rensselaer Polytechnic Institute, Troy, New York 12180, United States
3) Department of Chemical and Biological Engineering, Rensselaer Polytechnic Institute, Troy, New York 12180, United States
4) Fraunhofer IGB, Straubing Branch BioCat, Schulgasse 23, 94315, Straubing, Germany
5) TUM Catalysis Research Center, Ernst-Otto-Fischer-Straße1, 85748, Garching, Germany
6) The University of Queensland, School of Chemistry and Molecular Biosciences, 68 Copper Road, St. Lucia, 4072, Australia
7) Institute for Molecular Microbiology and Biotechnology, Westfälische Wilhelms-Universität Münster, Corrensstrasse 3, 48149 Münster, Germany

Corresponding author: jochen.schmid@uni-muenster.de

Keywords: *Paenibacillus polymyxa*. CRISPRa, CRISPRi, Cas12a, Multiplex gene regulation

Abbreviations: CRISPR: clustered regularly interspaced short palindromic repeats; CRISPRi: CRISPR interference; CRISPRa: CRISPR activation; gRNA: guide RNA; GTi: initiating glycosyltransferase; 2,3-BDL: 2,3-butanediol; EPS: exopolysaccharide

Abstract

Transcriptional perturbation using inactivated CRISPR-nucleases (dCas) is a common method in eukaryotic organisms. While rare examples of dCas9 based tools for prokaryotes have been described, multiplexing approaches are limited due to the used effector nuclease. For the first time, a dCas12a derived broad host range tool for the targeted activation and repression of genes was developed. Therefore, a previously described SoxS activator domain was linked to dCas12a to enable programmable activation of gene expression. Proof of principle of transcriptional regulation was demonstrated based on fluorescence reporter assays using the alternative host organism *Paenibacillus polymyxa* as well as *Escherichia coli*. Single target and multiplex CRISPR interference targeting the exopolysaccharide biosynthesis of *P. polymyxa* was shown to emulate polymer compositions of gene knock-outs. Simultaneous expression of 11 gRNAs targeting multiple lactate dehydrogenases and a butanediol dehydrogenase resulted in decreased lactate formation, as well as an increased butanediol production in microaerobic fermentation processes. Even though Cas12a is more restricted in terms of its genomic target sequences compared to Cas9, its ability to efficiently process its own guide RNAs *in vivo* makes it a promising tool to orchestrate sophisticated genetic reprogramming of bacterial cells or to screen for engineering targets in the genome. The developed tool will accelerate metabolic engineering efforts in common synthetic bacterial cell factories such as *E. coli,* as well as promising alternative host organisms.

1. Introduction

Seeking a biobased and sustainable economy, bacterial cell factories have been used for the production of a variety of high value products such as amino acids[1], biofuels[2] or biosynthesis of complex pharmaceutical compounds like artemisinic acid[3]. The

development of robust production strains for industrial scale production typically requires a deep understanding of the underlying metabolic networks enabling sophisticated engineering technologies to optimize fluxes towards the product of interest and eliminating unwanted side products[4]. Within the last decade, the development of new technologies such as CRISPR-Cas9 mediated genome editing resulted in a dramatic increase in the complexity and scope of metabolic engineering approaches[5–8].

Catalytically inactive variants of CRISPR-nucleases (dCas), which still bind specific DNA sequences via programmable guide RNAs (gRNA) but do not cause a double strand break, have been applied to physically block gene expression in a multitude of CRISPR interference (CRISPRi) approaches in bacteria[9–11] modulating the expression of genes of interest. In eukaryotic organisms, CRISPRi has been further expanded by direct fusion of Cas9 and effector domains to remodel the chromatin structure of target genes resulting in an even tighter control of expression[12–14]. Contrary, CRISPR-mediated activation (CRISPRa) of gene expression was achieved by linking the deactivated CRISPR-nuclease from *Streptococcus pyogenes* dCas9 to transcriptional activation domains via translational fusion or recruitment domains on the target gRNA[15,16]. While CRISPRa has been extensively used and further developed for eukaryotic organisms to activate transcription of target genes[17], the number of synthetic tools for prokaryotes is still limited. Recently, new CRISPR-Cas9 based systems were developed for bacteria using effector domains such as RpoZ[9], RpoA[18,19], bacteriophage derived transcriptional activators like AsiA[20,21] or the more effective AraC family transcription factor SoxS[22] that facilitate the recruitment of the RNA polymerase holoenzyme. In order to overcome narrow target site requirements, more flexible CRISPRa toolkits using σ^{54}-dependent promoters were established[23]. Thereby,

CRISPR-dCas guided bacterial enhancer binding proteins were directed to upstream activating sequences in order to enable long distance regulation of target promoters. Similar to eukaryotic systems, a remarkable dynamic output range was achieved[23].

While Cas9 derived from *Streptococcus pyogenes* is the most well-studied RNA-guided endonuclease and was used in a multitude of studies, it has demonstrated several downsides in simultaneously targeting multiple loci. Although, multiplex genome editing can be realized, a uniform expression of multiple gRNAs proved to be challenging. Strategies to overcome this constraint include the expression of sgRNA transcripts from multiple plasmids, the co-expression of RNA processing enzymes such as RNAse III[24] and Csy4[25,26] or flanking of consecutive gRNAs by ribozymes or tRNAs that enable efficient processing of the mature gRNA[27,28] from a single transcript. However, all these strategies are limited in the number of multiplex targets due to cytotoxic effects. Contrary, multiplex genome editing approaches using Cas12a nuclease orthologs (also known as Cpf1) from *Francisella novicida, Acidaminococcus* sp. or *Lachnospiraceae* sp. require only the expression of a single crRNA array[29,30]. Opposed to Cas9, these minimalistic class 2 type V-A CRISPR-Cas systems do not contain the HNH nuclease domain. Instead, the staggered double strand cleavage of the target DNA is mediated by a single RuvC domain upon binding of the ribonucleoprotein complex to its target site[31,32]. Interestingly, unlike Cas9, Cas12a additionally possesses RNase activities to process the precursor crRNA array and form the gRNAs necessary to direct the CRISPR nuclease to the target DNA[30]. Leveraging this dual RNase/DNase function, simultaneous perturbation of 25 individual targets was demonstrated in mammalian cell lines using a single transcript harboring both the open reading frame of Cas12a and a CRISPR array[33]. The protospacer adjacent motif (PAM), required for CRISPR-nucleases to bind and cleave its target DNA, of Cas12a

nucleases differs from Cas9. Contrary to Cas9, the PAM is located upstream of the cleavage site and consists of a sequence with a very low GC content. For all commonly used Cas12a nucleases from *Francisella novicida, Acidaminococcus* sp. or *Lachnospiraceae* sp. the most efficient PAM was determined as TTTV[34,35]. While this particular PAM is more restrictive compared to NGG of *Sp*Cas9, protein engineering efforts to loosen the stringency of CRISPR nucleases to enable genome editing in otherwise inaccessible loci were successful[36,37].

Due to its advantages for multiplex genome perturbation studies, dCas12a has been extensively used for the tunable transcriptional regulation of gene expression via CRISPRi and CRISPRa in eukaryotic cells[29,33,37]. Despite rapid advances in CRISPR-based technologies, to the best of our knowledge, only CRISPR interference studies have previously been reported for prokaryotic cells using dCas12a[38], while publications demonstrating the targeted gene activation via CRISPRa are still missing for this promising CRISPR system. Therefore, the aim of this study was to establish a functional dCas12a based multiplex gene modulation system capable of CRISPRa and CRISPRi using a broad-host range plasmid.

Paenibacillus polymyxa is a Gram-positive, spore forming, non-pathogenic, soil bacterium[39] of biotechnological interest for its ability to produce enantiopure *R,R*-2,3-butanediol (2,3-BDL) and exopolysaccharides (EPS) with interesting material properties[40,41]. *P. polymyxa* DSM 365 putatively produces two distinct heteroexopolysaccharides we termed Paenan I and Paenan II, which is reflected in two functionally complete EPS clusters encoding all genes required for the Wzx/Wzy biosynthesis pathway[42,43]. Knock-outs of distinct glycosyltransferases within the clusters resulted in EPS variants with altered rheological behavior[42]. While more laborious and time consuming knock-outs can be conducted, CRISPRi-based knock-

downs might be used to enable the fast screening of new EPS variants with interesting material properties. *P. polymyxa* is also applied in the production of 2,3-BDL via the mixed-acid fermentation pathway in microaerobic conditions. Depending on oxygen availability, production of side products such as lactate, formate and ethanol is required to maintain the redox balance[44]. We recently showed that metabolic engineering of the side pathways competing for pyruvate was able to increase productivity of 2,3-BDL biosynthesis[45]. However, despite the knock-out of one specific lactate dehydrogenase, lactate as a by-product was still produced due to the action of redundant homologs. In this study, lactate should be eliminated by the concerted knock-down of all four different lactate dehydrogenases found in the genome. Additionally, the carbon flux should be directed towards 2,3-BDL by inducing the expression of the butanediol dehydrogenase in parallel via a newly developed CRISPRa/i system.

2. Materials and Methods

2.1 Strains and media

P. polymyxa DSM 365 was acquired from the German Collection of Microorganisms and Cell Culture (DSMZ), Braunschweig, Germany. *E. coli* NEB Turbo cells (New England Biolabs, USA) were used for any plasmid construction presented in this study. *E. coli* S17-1 (DSMZ strain DSM 9079) was utilized for transformation of *P. polymyxa* DSM 365 via conjugation. All medium components were obtained from Carl Roth GmbH (Germany) if not indicated differently. For cloning procedures, strains were grown in LB media (5 g L^{-1} yeast extract, 10 g L^{-1} tryptone, 10 g L^{-1} NaCl) and additionally supplemented with 50 µg mL^{-1} neomycin and 20 µg mL^{-1} polymyxin if required. All strains were stored in 30 % glycerol at -80 °C. Prior to cultivation, strains were streaked on LB agar plates and grown at 30 °C. All strains used or constructed in this study are listed in Table S1.

For 2,3-BDL fermentations a single colony was used for inoculation of 50 mL pre-culture medium containing 60 g L^{-1} glucose, 5 g L^{-1} yeast extract, 5 g L^{-1} tryptone, 0.2 g L^{-1} $MgSO_4$ heptahydrate (Sigma Aldrich, USA), 3.5 g L^{-1} KH_2PO_4, 2.5 g L^{-1} K_2HPO_4. Fermentation medium components were autoclaved separately and contained 120 g L^{-1} glucose, 5 g L^{-1} yeast extract, 3.5 g L^{-1} tryptone, 0.2 g L^{-1} $MgSO_4x7$ H_2O, 3.5 g L^{-1} KH_2PO4, 2.5 g L^{-1} K_2HPO_4, 5 g L^{-1} ammonium acetate, 4 g L^{-1} $(NH_4)_2SO_4$ and 3 mL L^{-1} trace element solution. Trace element solution contained 2.5 g L^{-1} iron sulfate heptahydrate, 2.1 g L^{-1} sodium tartrate dihydrate, 1.8 g L^{-1} manganese chloride dihydrate, 0.075 g L^{-1} cobalt chloride hexahydrate, 0.031 g L^{-1} copper sulfate pentahydrate, 0.258 g L^{-1} boric acid, 0.023 g L^{-1} sodium molybdate dihydrate and 0.021 g L^{-1} zinc chloride. Trace element solution was filter-sterilized and added to the media after cooling down to room temperature.

For EPS production, MM1 P100 medium[40] was used as described before, containing 30 g L^{-1} glucose and 5 g L^{-1} peptone. The corresponding pre-culture medium contained a reduced amount of 10 g L^{-1} glucose and was buffered to pH 6.8 with 20 g L^{-1} MOPS.

2.2 Plasmid construction

The gene encoding for an engineered (E174R, N282A, S542R, K548R)[37] catalytically inactivate (D908A) variant of AsCas12a was codon optimized for *Bacillus* ssp. and synthesized by ATG:biosynthetics (Germany). The basic plasmid pCRai (Figure S1) was assembled by isothermal Gibson Assembly[46] from three PCR-amplified fragments consisting of a pUB110 derived backbone including oriT for conjugational transfer[42], a lacZ replacement cassette for BbsI based cloning of target gRNAs and the codon optimized *enAsdcas12a* cassette. Activator domains were PCR-amplified from extracted gDNA of *P. polymyxa* DSM 365 and *E. coli* NEB Turbo respectively and cloned into pCRai by Golden Gate Assembly using BsaI. Cloning of gRNA sequences

was conducted as previously described[42]. The PsgsE-sfGFP reporter was cloned via isothermal Gibson Assembly using a unique SpeI site of pCRai. The dual reporter plasmid was constructed by cloning a PsgsE-mRFP and a PsgsE-sfGFP reporter cassette in tandem by Golden Gate Assembly after linearization of pCRai_soxS with SpeI/SalI. All oligonucleotides used for the construction of plasmids are listed in Table S2 and S3.

2.3 Conjugation based transformation of *P. polymyxa* DSM 365

P. polymyxa was transformed by conjugation using *E. coli* S17-1 harboring the various plasmids. Overnight cultures of donor and recipient strains were diluted 1:100 with selective or non-selective LB media respectively and cultivated at 37 °C for 3 h, 280 rpm. 900 µL of the recipient culture was heat shocked at 42 °C for 15 min and mixed with 300 µl of the donor strain culture. Cells were centrifuged at 6,000 g for 2 min, resuspended in 800 µl LB media and dropped on non-selective LB agar plates. After 24 h of incubation at 30 °C, cells were scrapped off, resuspended in 500 µl LB-broth and 100 µl thereof plated on selective LB-agar containing 50 µg mL^{-1} neomycin and 20 µg mL^{-1} polymyxin for counter selection. *P. polymyxa* conjugants were analyzed for successful transformation after 48 h incubation at 30 °C by cPCR. Confirmed knock out strains were plasmid cured by cultivation in LB broth without antibiotic selection pressure and subsequent replica plating on LB agar plates both with and without neomycin. Strains that did not grow on plates with selection marker were verified by sequencing of the target region and used for further experiments.

2.4 Photometric assay

For sfGFP fluorescence experiments, 3 mL of EPS medium supplemented with 50 µg mL^{-1} neomycin was inoculated with a single colony of the respective strains and grown

over night at 37 °C, 200 rpm. After 18 h, each strain was sub-cultured 1:100 in 3 mL selective MM1 P100 medium and grown for 24 h at 37 °C, 200 rpm. After 24 h, 100 µl were transferred to a 96 well microtiter plate and OD_{600}, GFP fluorescence (Ex. 488 nm Em. 515 nm) and mRFP fluorescence (Ex. 560 nm Em. 600 nm) measured in a Ultraspec 10 spectrophotometer (Amersham Biosciences, UK). In parallel, 1 mL of each culture was pelleted by centrifugation and used for qPCR experiments.

2.5 Quantitative RT-PCR

RNA extraction of positive samples of the GFP fluorescence assay as well as butanediol fermentation processes was performed using the Aurum Total RNA Mini Kit (BioRad, USA) according to the manufacturer's instructions. Synthesis of cDNA was conducted using iScript reverse transcriptase (BioRad, USA) using 1 µg total RNA template. The qPCR reactions were performed in triplicates on a CFX-96 thermocycler using SsoAdvanced Universal SYBR Green Supermix (BioRad, USA) using 5 ng of cDNA as a template in 10 µl reaction volume. Negative controls without reverse transcriptase during cDNA synthesis were used in order to evaluate the absence of gDNA contaminations. Relative gene expression levels were calculated based on the ΔΔCq method[47] and *gyrA* as a reference gene. After qPCR, a melting curve analysis was performed to confirm the presence of a single PCR product for each target. Designed primers were analyzed by the OligoAnalyzer Tool (IDT, USA) to avoid hairpin formation, self- and hetero dimer formation with free energy values more than 10 kcal mol^{-1}. Oligonucleotides used for qPCR experiments are listed in Table S2.

2.6 CRISPR-Cas9 mediated genome editing

All gene knock-outs were performed as previously described by Rütering et al.[42]. In brief, gRNAs for the targeted genome regions were designed using Benchling CRISPR Design Tool. For each target a minimum of two gRNAs were designed typically

targeting distinct regions of the open reading frame. Oligonucleotides were phosphorylated, annealed and cloned into pCasPP by Golden Gate assembly. Approximately 1 kB up- and downstream homology flanks for each targeted nucleotide sequence were amplified from genomic DNA of *P. polymyxa* DSM 365 using Phusion Polymerase according to the manufacturer's instructions and fused by overlap extension PCR via a 20 bp overlap. Homology flanks were cloned into pCasPP through Gibson Assembly or molecular cloning after linearization by use of SpeI. After transformation of *E. coli* NEB Turbo, clones were analyzed for correct construct assembly by colony PCR (cPCR) and sequencing of the amplicons. Finally, correct constructs were transferred to chemical competent *E. coli* S17-1 cells for the following conjugational transformation of *P. polymyxa*.

2.7 EPS batch fermentation

EPS fermentations were conducted in a 1 L DASGIP parallel bioreactor system with a working volume of 500 mL. A single colony from a freshly streaked plate was used to inoculate 100 mL MM1 P100 pre-culture medium by following incubation for 16 h at 30 °C, 160 rpm. Bioreactors were inoculated to give an initial OD of 0.1. Fermentation was performed at 30°C and stirrer speed (200 - 600 rpm) and gassing (6 - 10 L h^{-1}) with pressurized air through a L-sparger were controlled to maintain 30 % DO saturation. The stirrer was equipped with a 6-plate-rushton impeller placed 2.5 cm from the bottom of the shaft. The pH value was maintained at 6.8 and automatically adjusted with 2 M NaOH or 1.35 M H_3PO_4 as required. Foam control was performed using 1 % of antifoam B (Merck, Germany). For monitoring the process parameters, reactors were equipped with redox and dissolved oxygen probes.

After the end of the process the fermentation broth was diluted 1:10 with dH_2O and the biomass was separated by centrifugation (15 000 g, 20°C, 20 min) followed by cross-

flow filtration of the supernatant using a 100 kDa filtration cassette (Hydrosart, Sartorius AG, Germany). EPS was precipitated by slowly pouring the concentrated fermentation supernatant into two volumes of isopropanol. EPS was collected and dried overnight in a VDL53 vacuum oven at 40°C (Binder, Germany). Dry weight of the obtained EPS was determined gravimetrically prior to milling to a fine powder in a ball mill at 30 Hz for 1 min (Mixer Mill MM400, Retsch GmbH, Germany).

2.8 Carbohydrate fingerprinting

EPS monosaccharide composition was analysed using the 1-phenyl-3-methyl-5-pyrazolone high-throughput method (HT-PMP) as previously described using 1 g L^{-1} reconstituted EPS solutions[48]. In brief, 0.1 % EPS solutions were hydrolyzed in a 96 well plate, sealed with a rubber mat and further covered by a custom-made metal device with 2 M TFA (90 min, 121°C). Samples were neutralized with 3.2 % NH_4OH. 75 µl of PMP master mix (125 mg PMP, 7 mL MeOH, 3,06 mL dH_2O, 437.5 µL 3.2% NH_4OH) were mixed with 25 µl of neutralized hydrolysate and incubated at 70°C for 100 min in a PCR cycler. 20 µl of derivatized samples were mixed with 130 µl of a 1:26 dilution of 0.5 M acetic acid and filtered with a 0.2 µm filter plate (1,000 g, 2 min) followed by HPLC-UV-MS analysis as previously described[48].

2.9 Butanediol batch fermentation

Batch fermentations were conducted in 1 L DASGIP bioreactors (Eppendorf, Germany) with an initial volume of 550 mL. A single colony from a freshly streaked plate was used to inoculate 100 mL pre-culture medium by following incubation for 16 h at 30 °C, 160 rpm. 50 mL of this cultivation broth (diluted with pre-culture medium if required) were used to inoculate the bioreactor by an initial OD_{600} of 0.1. Fermentation was performed at 35 °C and constant aeration of 0.075 vvm. The stirrer was equipped with a 6-plate-rushton impeller placed 4 cm from the bottom of the shaft and constantly stirring at 300

rpm. The pH value was maintained at 6.0 and automatically adjusted with the addition of 2 M NaOH or 1.35 M H_3PO_4 as required. Foam control was performed using 1 % of antifoam B (Merck, Germany). In order to monitor process parameters, reactors were equipped with redox and pH probes. Glucose and product concentrations were determined via a HPLC-UV-RID system (Dionex, USA) equipped with Rezex ROA-H^+ organic acid column (300 mm x 7.8 mm Phenomenex, USA). Column temperature was set to 70 °C and 2.5 mM H_2SO_4 was used as the mobile phase with a flow rate of 0.5 ml min^{-1}. All measured concentrations of 2,3-BDL in this publication represent solely the levo-stereoisomer of the alcohol if not explicitly noted differently.

3. Results and Discussion

3.1 Identification of functional transcriptional activator domains

In a first step, different transcription activator domains of distinct regulatory protein families were tested in order to identify a suitable candidate for CRISPRa. Each domain was linked by translational fusion to the C-terminal end of dCas12a through a 10 amino acid flexible linker peptide (-GSEASGSGRA-). As endogenous transcription activators from *P. polymyxa,* the cAMP receptor protein (CRP) RNA polymerase subunits σ^{70} (RpoD) and ω (RpoZ), as well as the regulator of the glutamate synthase operon (GltC) were evaluated. SoxS, an activator of the superoxide stress genes from *E. coli* was chosen as an additional heterologous regulator. Out of these, only RpoZ and SoxS have previously been reported as suitable candidates using dCas9 based CRISPRa systems[9,22]. The plasmid pCRai_sfGFP was constructed by isothermal assembly based on the previously established Cas9 genome editing plasmid pCasPP[42]. pCRai_sfGFP encodes dCas12a linked to the different transcriptional activators, the

corresponding gRNA expression cassette, as well as *sfgfp* under the control of constitutive promoters.

The sgsE-promoter from *Geobacillus stearothermophilus* used for sfGFP expression is a temperature sensitive promoter containing three core promoter sites[49]. At low temperatures of 28 °C the front most core promoter (P3) is active, resulting in a weak basal expression, while elevated temperatures of 37 - 45°C lead to highly increased expression from RNA-polymerase binding sites further upstream (P1 and P2) as shown in *B. subtilis*[49]. Therefore, this promoter was chosen to test CRISPRa activities of the different activator domains in order to induce strong expression levels even at low temperature (Figure 1 A). Eukaryotic CRISPRa systems allow a relatively broad range, in which gRNAs mediate the binding of the CRISPR effector module to efficiently activate or repress the expression of target genes. Contrarily, bacterial CRISPRa systems have demonstrated to be highly sensitive to the correct distance of the gRNA binding site to the promoter[22]. Bacterial CRISPRa systems act by facilitating the recruitment of the RNA-polymerase to the promoter, while eukaryotic systems typically cause chromatin re-arrangements to interfere with the expression of target genes[13]. For bacterial dCas9 based systems, an optimal distance was determined in the range between 60 to 100 bp upstream of the transcriptional start site (TSS)[22]. The optimal distance might vary depending on different activator domains. Consequently, we tested four different gRNAs binding to the template and non-template strand in the range of 40 to 120 bp upstream of the TSS to induce expression from the strong RNA-polymerase binding site P3 (Figure 1). In order to test whether observed effects actually arise from the binding of the dCas12a-activator complex to the respective target sites, additional constructs with off-target gRNAs expression were constructed.

Out of all tested gRNA-activator constructs, *Ec*SoxS demonstrated the best performance in *P. polymyxa* (Figure 1 B). Three out of four tested gRNAs significantly increased expression of sfGFP and showed an increased fluorescence signal during photometric evaluation. The qPCR experiments showed up to 6.5-fold increased transcription levels for gRNA_a4, but also gRNA_a1 and gRNA_a3 displayed increased transcription and fluorescence signals (Figure 1 C). Surprisingly, the highest fluorescence signal was achieved using gRNA_a4, which was positioned 50 bp upstream of the TSS of the heat-inducible promoter site P1 (Figure 1 A). While the close proximity of the binding site of this gRNA lies outside of the ideal distance determined for a dCas9-soxS construct[22], the distance to the second RNA-polymerase binding site (P2) of 85 bp might result in transcription from the secondary heat-inducible promoter.

Additionally, dCas12a fused to other activator domains such as RpoD, GltC and CRP respectively also demonstrated increased fluorescence results for individual gRNAs (Figure 1 B). However, some combinations also led to a decreased fluorescence signal of GFP in *P. polymyxa* indicating that the effector module blocks the binding of the RNA-polymerase to the promoter and therefore effectively represses transcription of the gene of interest. For GltC and CRP, the use of gRNAs a3 and a4, which are located in close proximity to each other (10 bp), effects on GFP expression changed from 2-fold increased GFP signal to transcriptional repression. All of the investigated activators act by direct interaction with the RNA-polymerase[50–52]. Contrary to other activators, there is experimental evidence suggesting that SoxS already forms a binary pre-recruitment complex with the C-terminal domain of the α-subunit and scans DNA for cognate SoxS binding sites[53,54]. Therefore, we hypothesize that a similar pre-recruitment is formed with the dCas12a-SoxS fusion protein, which allows more

352 flexibility in the correct distancing of the gRNA to the promoter binding site. Due to the
353 consistent performance of the dCas12a-soxS constructs, this particular activator
354 domain was used for all further experiments.

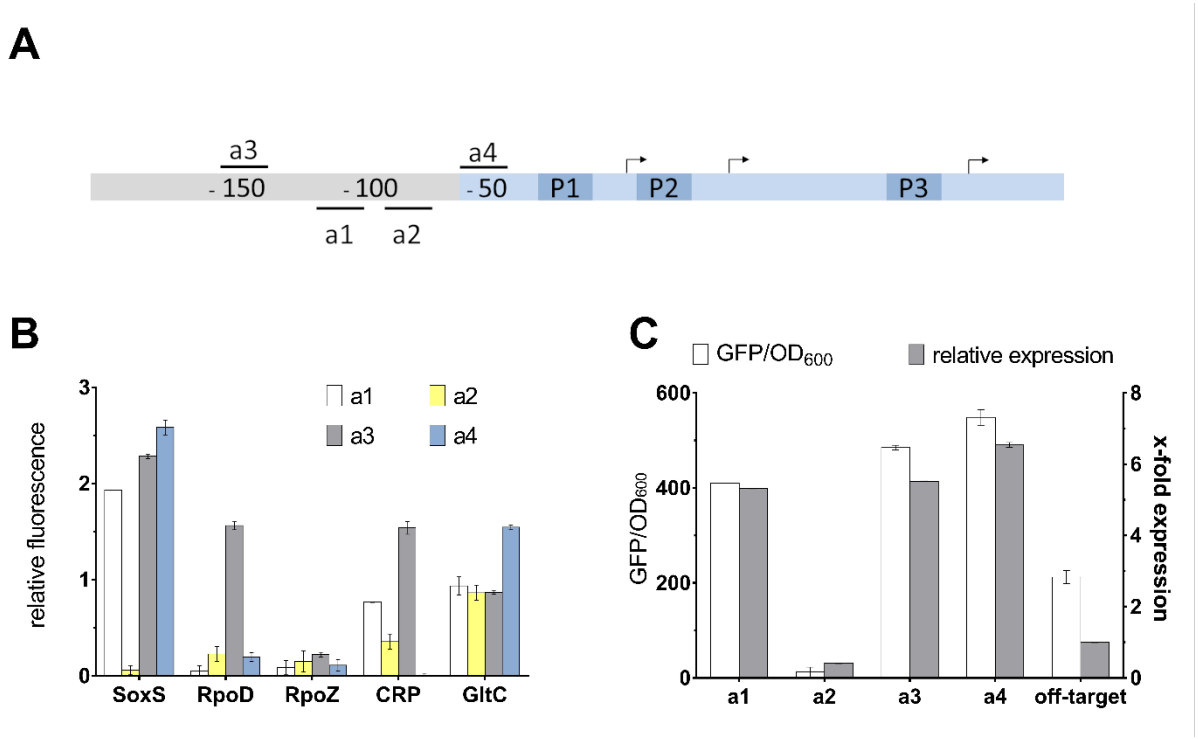

355

356 **Figure 1: Establishment of a CRISPRa system using dCas12a linked to activator**
357 **domains** A) Schematic overview of CRISPRa target sites upstream of the *sgsE*
358 promoter (blue). dCas12a was fused to different activator domains (SoxS, RpoD,
359 RpoZ, CRP, GltC) and positioned upstream of the *sgsE*-promoter with multiple gRNAs
360 targeting template and non-template strand (a1 - a4). The promoter consists of three
361 core promoter binding sites (P1 - P3), of which the heat-inducible P1 site corresponds
362 to the strongest expression[49]. CRISPRa experiments aim to activate expression from
363 P1 already at low temperatures. Arrows indicate the TSS of the corresponding core
364 promoter sites. B) GFP expression using different activator domains and gRNAs (a1 -
365 a4) relative to a corresponding off-target gRNA. SoxS showed up to 2.5-fold GFP
366 fluorescence with three gRNAs, while RpoD, CRP and GltC demonstrated elevated
367 fluorescence for only one gRNA respectively. C) Expression levels determined by
368 qPCR (relative expression) showed up to 6.5-fold increased transcription levels of *gfp*
369 for soxS variants compared to off-target gRNAs.

Interestingly, while all experiments using the fluorescence reporter system were performed in *P. polymyxa*, observed effects were almost identical in *E. coli* S17-1 that was used for the conjugational transformation of *P. polymyxa* DSM 365 (Figure S 2). Consequently, we demonstrated a broad-host range use of the constructed pCRai_soxS plasmid in both Gram-positive, as well as Gram-negative bacteria. In case of the fluorescence reporter assays, in which all functional parts were encoded on a single plasmid, it was possible to accelerate the screening of potential guide RNAs by using *E. coli* S17-1 as a pre-screening platform prior to the more time-consuming conjugational transformation of *P. polymyxa* DSM 365.

Our results exemplified that the stringency of gRNA positioning with the SoxS domain is lower compared to other activators. Empirical testing of multiple gRNAs is still required to enable improved activation of target promoters. However, it might be possible to establish a design rule set to enable *a priori* construction of optimized gRNAs with more experimental data using different promoters.

3.2 Establishment of CRISPRi and multiplexing CRISPRi/a

In a next step, we evaluated whether the use of the dCas12a-soxS activator constructs is also possible for CRISPRi by re-positioning the gRNA within the open reading frame of sfGFP. Thereby, the effector module acts as a road block for the RNA-polymerase and inhibits the elongation of the nascent transcript. Three different gRNAs binding sites were tested (Figure 2 A). While expression levels of *sfgfp* were significantly decreased by approximately 80 % for all constructs, the actual fluorescence of GFP remained at higher levels for gRNAs T1 and T2 (Figure 2 A B). Even though, fluorescence signals were not fully eliminated, a severe decrease of up to 95 % for gRNA T3 was observed.

A

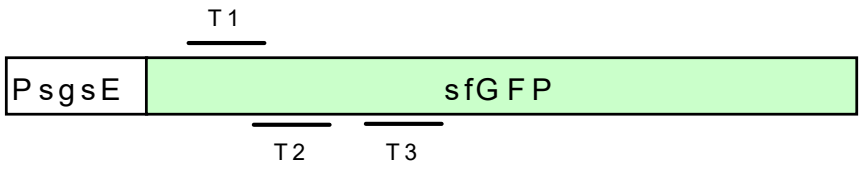

B

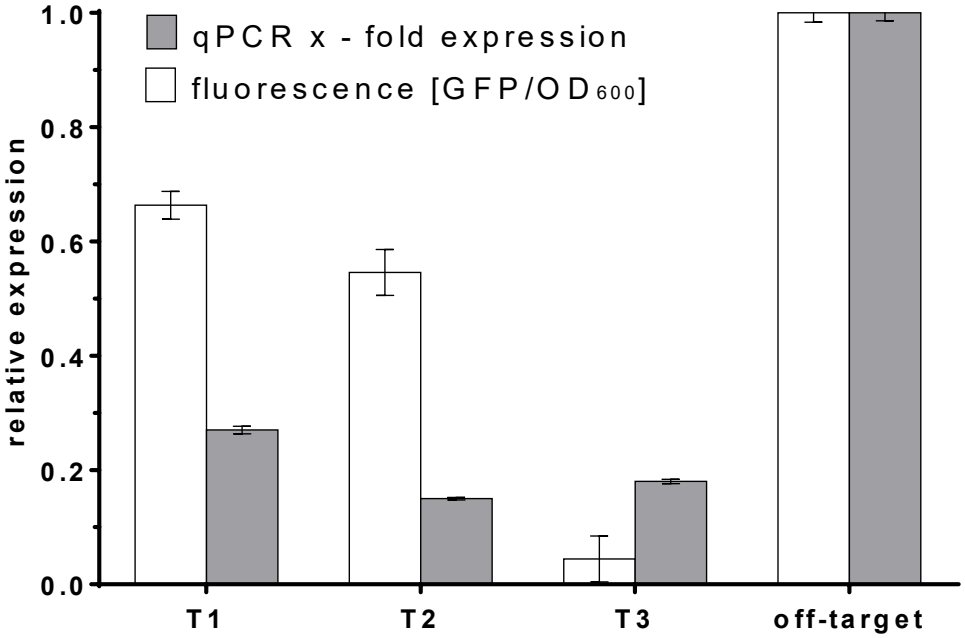

394

395 **Figure 2: Establishment of CRISPRi in *P. polymyxa* using pCRai_soxS**. A)
396 Schematic overview of gRNA binding sites within the ORF of sfGFP. B) Three gRNAs
397 targeting the ORF of *sfgfp* (T1-T3) were tested respectively by fluorescence
398 experiments and qPCR expression analysis relative to an off-target gRNA. While
399 transcriptional expression levels were reduced by 75 % to 80 % for all gRNAs,
400 measured fluorescence levels of GFP fluctuated more between different gRNAs. The
401 gRNA T3 demonstrated the best repression resulting in a highly reduced fluorescence
402 signal as well as a reduced transcription of *sfgfp*. Reporter expression was determined
403 photometrically and by qPCR experiments in biological triplicates.

404

In order to test the capability of our construct to simultaneously repress and activate different target genes, a continuously expressed mRFP reporter cassette was cloned in pCRai_soxS in addition to the sfGFP reporter. For CRISPRa, the previously used gRNA_a1 was chosen to induce the expression of sfGFP. For CRISPRi a new gRNA was designed binding within the ORF of *mrfp* (Figure 3 A*)*. All strains of *P. polymyxa* were compared to a strain harboring an off-target CRISPR-array. Due to weak fluorescence signals after 24 h of inoculation, only transcriptional expression levels were determined via qPCR at this point of time, but photometric evaluation of the reporters was performed after 48 h. When expressed individually, CRISPRi resulted in a reduction of the mRFP fluorescence signal by 74 %, while CRISPRa increased sfGFP expression by 68 % (Figure 3 B). Simultaneous expression of both gRNAs from a single CRISPR-array decreased mRFP fluorescence by 60 %, while increasing the fluorescence signal of sfGFP by 120 %. Therefore, we demonstrated the efficient control of the expression of multiple genes using a single CRISPR-array. Depending on the positioning of the gRNAs, it prooved possible to activate or repress multiple target genes in parallel.

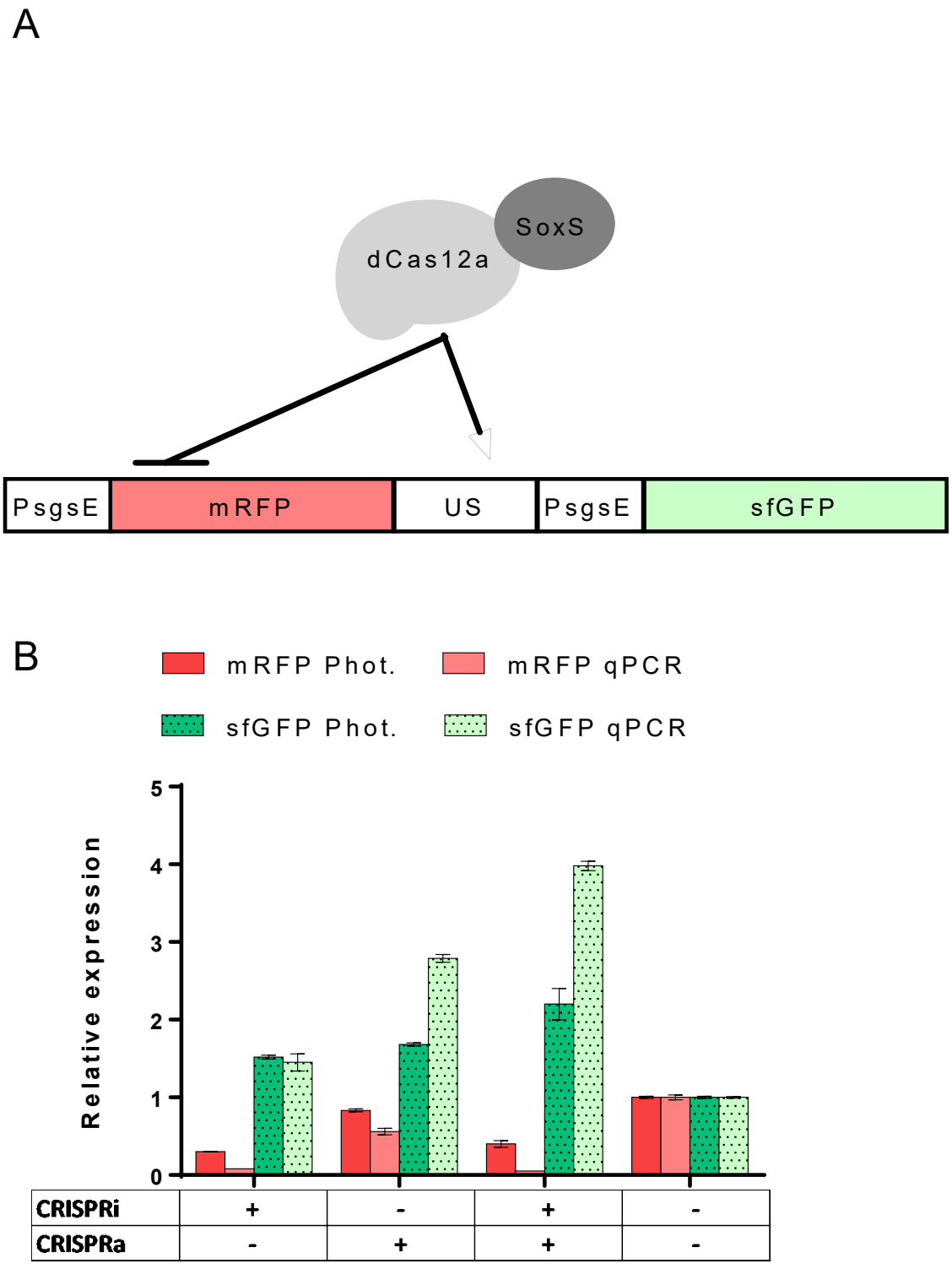

421

422 **Figure 3: Simultaneous repression (CRISPRi, mRFP) and activation (CRISPRa,**
423 **sfGFP) of fluorescence reporters**. A) Schematic display of gRNA binding sites within
424 the ORF of mRFP and in the upstream region (US) of PsgsE controlling the expression

of sfGFP. B) Multiplex transcriptional perturbation was tested in *P. polymyxa* harboring a plasmid for the constitutive expression of GFP and mRFP fluorescence reporters. Single CRISPR arrays were designed targeting the ORF of mRFP or the upstream region of PsgsE controlling *sfgfp* expression (gRNA_a1). Expression of gRNAs resulted in the repression of mRFP or induction of sfGFP respectively. When both gRNAs were expressed simultaneously, obtained fluorescence results were similar to the expression of individual gRNAs alone. All results are depicted relative to an off-target CRISPR array encoding a gRNA not present in the strain. Reporter expression was determined photometrically and by qPCR experiments in biological triplicates.

3.3 Multiplex CRISPRi to modify exopolysaccharide composition of *P. polymyxa* DSM 365

The most important advantage of Cas12a over the more commonly used Cas9 is the ability of the effector nuclease to process its own crRNA, allowing the simultaneous targeting of multiple loci through a single CRISPR-array[33].

P. polymyxa DSM 365 is an avid producer of different exopolysaccharides. Depending on process conditions, variable polymer-mixtures are produced[40]. However, it has also been shown that the engineering of a polysaccharide structure with modified physicochemical properties is feasible[42]. The underlying gene cluster contains the two so-called initiating glycosyltransferases (GTi) PepC and PepQ, which are putatively responsible for the initiation of the biosynthesis of two distinct polysaccharides (Figure 4 A). Contrary to the first polymer (Paenan I), the second polymer (Paenan II) initiated by PepQ contains the deoxyhexose fucose (unpublished data). To evaluate the effects of CRISPRi constructs on genomic targets, the GTi PepQ was targeted alone or in combination with PepC. Strains harboring the plasmids pCRaiS (pCRai_soxS encoding an off-target spacer), pCRaiS_pepQ (targeting the ORF of *pepQ*) and pCRaiS_pepCQ (targeting the ORFs of *pepC* and *pepQ*) were constructed and used

in EPS batch fermentations. Carbohydrate fingerprints of the obtained EPS were performed and compared to the respective knock-out strains (Figure 4 B).

Strains harboring the pCRaiS plasmid expressing an off-target CRISPR-array did not show altered EPS composition. When the second GTi *pepQ* was targeted, fucose diminished, indicating the absence of Paenan II in the EPS mixture. In a next step, both initiating GTs were targeted simultaneously. With both GTis down-regulated, no EPS at all was produced. In order to evaluate whether the observed effects actually resulted from interference with the respective target genes, knock-out strains of the respective target genes with a previously established CRISPR-Cas9 genome editing system[42] were constructed. Our experiments confirmed that the monomer composition was comparable to the respective CRISPRi variants (Figure 4 B). In the previous fluorescence reporter assays, reduced signal of mRFP and GFP respectively could still be detected in CRISPRi approaches. Contrary, for the glycosyltransferase targets, no significant differences in EPS composition were observed between the CRISPRi constructs and the knock-out strains, indicating a more efficient repression of the target genes in comparison to the fluorescence assays.

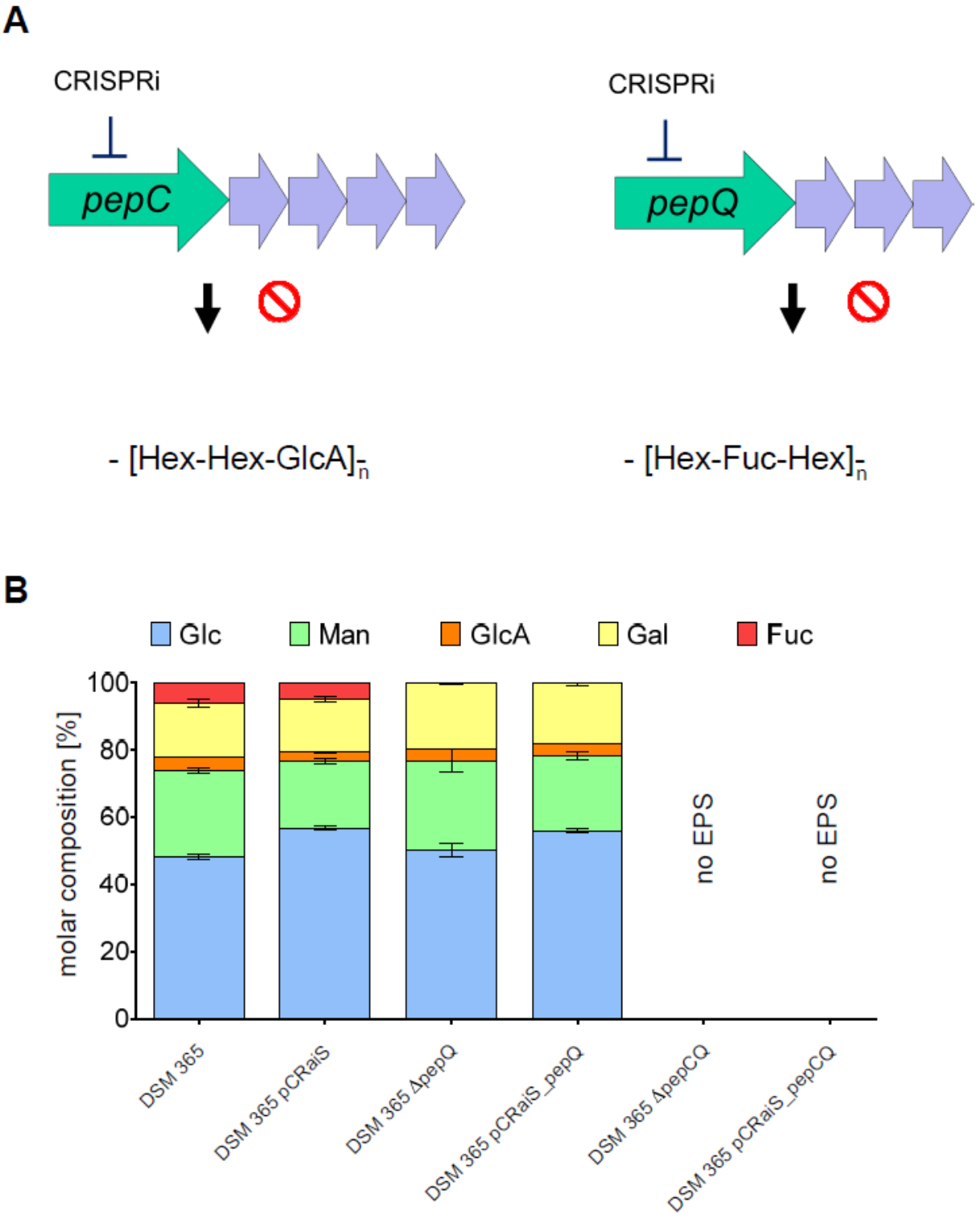

469

470 **Figure 4: Carbohydrate fingerprint of the heteroexopolysaccharide of *P.***
471 ***polymyxa* DSM 365 and engineered variants.** Transformation of *P. polymyxa* with a
472 plasmid encoding the SoxS activator domain and off-target gRNA (pCRaiS) did not
473 alter the EPS composition significantly. Expression of a gRNA targeting the ORF of the
474 initiating glycosyltransferase *pepQ* (pCRaiS_pepQ) resulted in the loss of fucose within

the EPS composition that was also observed in the KO strain *ΔpepQ*. Targeting the ORFs of both GTis (pCRaiS_pepCQ) did not yield any EPS resembling the same phenotype as the double KO *ΔpepCQ*, Δ: gene deletion by CRISPR-Cas9 mediated genome engineering. DSM 365: *P. polymyxa* DSM 365; pCRaiS: pCRai_soxS; Hex: hexose; GlcA: glucuronic acid; Fuc: fucose; Glc: glucose; Man: mannose; Gal: galactose

In conclusion, this approach showed that the developed pCRai_soxS tool can be used for the parallel screening for multiple interesting knock-out targets in the genome. In addition, the efficiency of this tool proved to be comparable to more laborious and time-consuming genome-editing approaches.

3.4 Multiplex CRISPRi/a to screen for metabolic engineering targets of the butanediol biosynthesis pathway in *P. polymyxa* DSM 365

In a previous study we engineered the mixed acid pathway of *P. polymyxa* DSM 365 to increase the production of 2,3-BDL and remove undesirable side-products. Interestingly, knock-out of a lactate dehydrogenase (*ldh1*) resulted in an adapted growth behavior, increased biomass formation and consequently enhanced 2,3-BDL formation[45]. However, due to the presence of additional homologs of *ldh* within the genome, lactate formation could not be completely eliminated. Therefore, in order to demonstrate the capabilities of our dCas12a-based CRISPR-tool, all additional copies of *ldh* homologs were targeted in parallel. Leveraging the CRISPR-array processing abilities of Cas12a, each gene was targeted with two gRNAs at the same time. As decoupling of the 2,3-BDL biosynthesis from its natural regulon showed positive effects, the expression of the butanediol dehydrogenase should also be transcriptionally activated in *P. polymyxa* DSM 365 *Δldh1*. Therefore, the corresponding promoter was predicted using the Softberry CNNPromoter_b tool[55]. Three distinct gRNAs positioned 106 - 180 bp upstream of the putative TSS were

501 tested separately (bdh_a1 – a3). Thereby, three strains carrying plasmid constructs,
502 each targeting 11 genomic sites in parallel were designed and evaluated in batch
503 fermentations using microaerobic conditions (Figure 5 A).

504

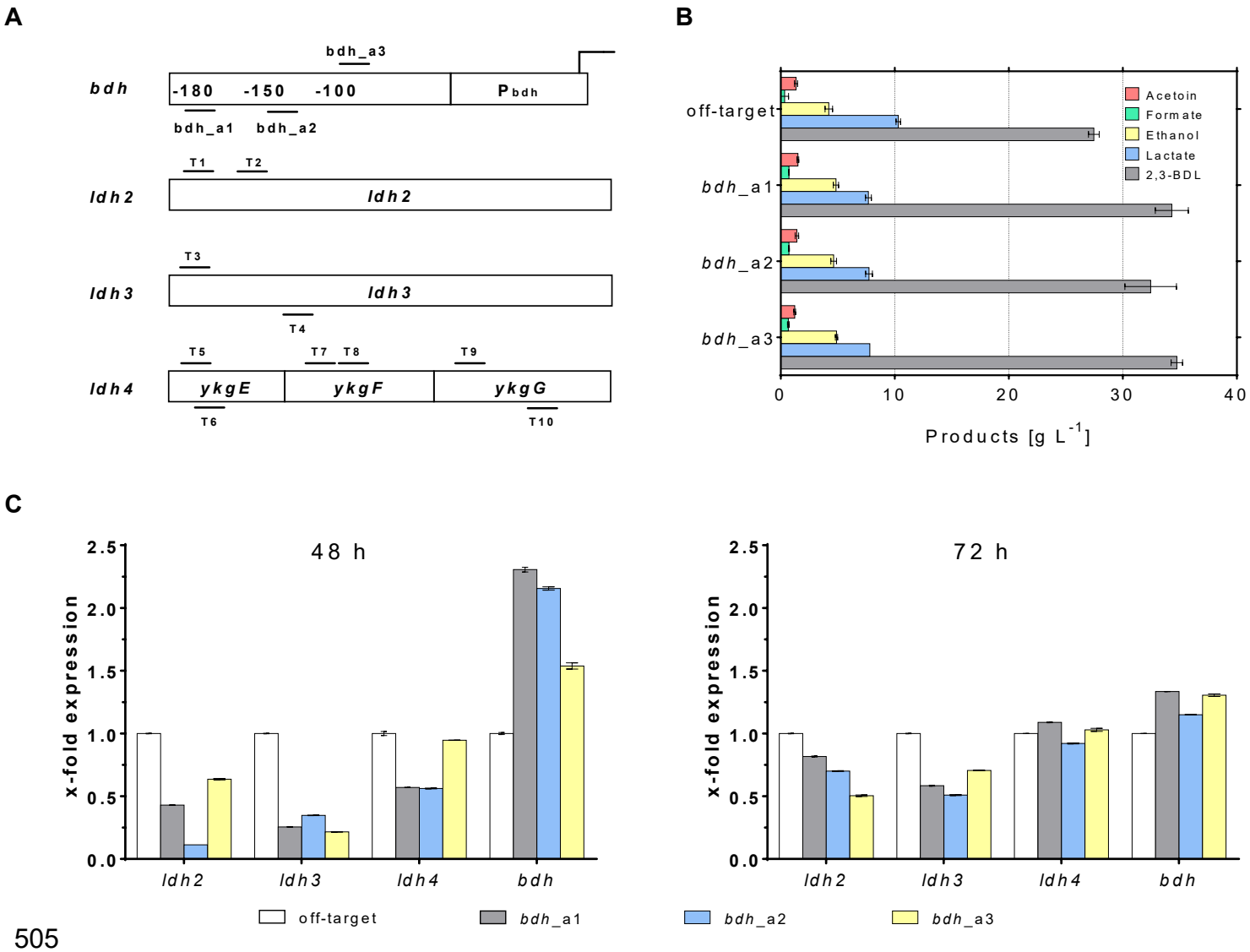

505

506 **Figure 5: Multiplex CRISPRi and CRISPRa to engineer the mixed acid pathway of**
507 ***P. polymyxa* and increase 2,3-BDL production**. A) Schematic overview of gRNA
508 binding sites. Three different gRNAs binding upstream of the P_{bdh} promoter were tested
509 individually (bdh_a1-3). Simultaneously, all constructs also targeted three putative
510 lactate dehydrogenase genes with a total of nine gRNAs (T1-T9) to knock-down the
511 respective genes. B) Product titer obtained after 72 h cultivation at microaerobic

conditions. Compared to an off-target construct, lactate production was reduced by ~20 % in strains expressing target gRNAs. 2,3-BDL production was increased and reached a maximum of 34.7 g L^{-1} in the construct using bdh_a3 to target *bdh* expression. Depicted values represent the mean of biological duplicates. C) Expression of target genes was analyzed via qPCR after 48 h and 72 h of cultivation. After 48 h, transcription levels of lactate dehydrogenases (*ldh*2 - 4) were significantly reduced compared to a strain expressing off-target gRNAs. Furthermore, also expression of a butanediol dehydrogenase was increased. However, after 72 h of cultivation, effects of CRISPRi and CRISPRa were severely reduced.

2,3-BDL fermentations were conducted for 72 h. Despite the fact that each ORF encoding the different lactate dehydrogenases was targeted with two gRNAs, lactate production in all strains was reduced only by ~20 % compared to the strain harboring the off-target gRNA (Figure 5 B). However, 2,3-BDL titers were increased from 27.5 g L^{-1} to 34.7 g L^{-1} for the *P. polymyxa* expressing gRNA bdh_a3, corresponding to a 26 % increased product titer. Additionally, also the strains encoding bdh_a1 and bdh_a2 showed 25 % and 18 % increased 2,3-BDL titers respectively. All other end products of the mixed acid pathway that were not targeted by any gRNA remained similar in all variants (Figure 5, Figure S 3). Furthermore, 2,3-BDL yields were increased by approximately 20 % for all strains encoding target gRNAs, indicating a redirection of the carbon flux from lactate to 2,3-BDL (Table S4).

While the general principle of our developed CRISPRi/a tool could be successfully demonstrated, effects of both transcriptional repression and activation were not as pronounced as observed in the fluorescence and EPS experiments. Expression analysis via qPCR revealed transcriptional perturbation of all *ldh* homologs ranging from 50 % to 80 % after 48 h of cultivation (Figure 5 C). Furthermore, two gRNAs binding 106 bp and 146 bp respectively upstream of the TSS of the *bdh* promoter

539 caused more than a 2-fold increased expression on the transcriptional level. However,
540 after 72 h effects on the transcriptional perturbation were significantly decreased. We
541 hypothesize that the observed decreased effects by our dCas12a tool are a combined
542 result of a rather low expression of the CRISPR-tool at microaerobic conditions and
543 long cultivation times used for 2,3-BDL fermentations. Due to the restrictive PAM site
544 of Cas12a of *Acidaminococcus* sp., optimal distancing from the TSS might not always
545 be possible and impede genome wide screenings. However, engineered variants of
546 Cas12a have shown expanded binding motifs and enabled the targeting of otherwise
547 inaccessible PAMs[37].

548 **4. Conclusion**

549 While CRISPRi has been continuously demonstrated in bacteria, CRISPRa technology
550 is lacking behind on their eukaryotic counterparts. Currently available systems are still
551 limited in their number of targets that can be modified in parallel due to the use of
552 dCas9. In this study, we showed the first successful utilization of dCas12a for the
553 simultaneous activation and repression of multiple genes in the alternative host
554 organism *P. polymyxa* DSM 365.

555 While gRNAs particularly for CRISPRa still need to be optimized individually for each
556 target promoter, utilization of SoxS as an activator domain enables more flexibility in
557 the correct distancing to the target promoter compared to other tested activator
558 domains. In this study, we demonstrated an efficient broad host range tool for the
559 parallel transcriptional modulation of expression patterns in bacteria that can be
560 applied for both metabolic engineering efforts and screening of potential targets for
561 further studies. With ongoing studies using dCas12a-SoxS based tools for CRISPRa
562 in bacterial hosts it will be possible to establish more precise design rule sets for the

563 efficient positioning of the effector module for CRISPRi and CRISPRa to facilitate and
564 accelerate the use of dCas12a based transcriptional perturbation tools.

565 Even though Cas12a is more restricted in terms of its PAM sequence compared to
566 Cas9, its ability to efficiently process its own gRNAs makes it a promising tool to
567 orchestrate sophisticated genetic reprogramming of bacterial cells or to screen for
568 engineering targets in the genome.

569 In conclusion, this work demonstrated both, the simultaneous activation and repression
570 of multiple targets in the genome of *P. polymyxa* using a single CRISPR array and
571 represents therefore an important extension of current Cas9-based tools. We
572 demonstrated that the developed tool is functional in common bacterial cell factories
573 such as *E. coli* as well as in the Gram-positive alternative host organism *P. polymyxa*.
574 Usage of multiplex transcriptional perturbation will facilitate genome wide screenings
575 of potential engineering targets and thereby accelerate metabolic engineering efforts.

576 **5. Acknowledgement**

577 This work was supported by the German Federal Ministry of Education and Research
578 (BMBF) in frame of the project MaPolKo (number 03VP02560). MAGK would like to
579 acknowledge funding from the U.S. National Science Foundation, award MCB-
580 1817631.

581

References

(1) Wendisch, V. F.; Bott, M.; Eikmanns, B. J. Metabolic Engineering of *Escherichia coli* and Corynebacterium Glutamicum for Biotechnological Production of Organic Acids and Amino Acids. *Curr. Opin. Microbiol.* **2006**, *9* (3), 268–274. https://doi.org/10.1016/j.mib.2006.03.001.

(2) Jin, Y.-S.; Cate, J. H. Metabolic Engineering of Yeast for Lignocellulosic Biofuel Production. *Curr. Opin. Chem. Biol.* **2017**, *41*, 99–106. https://doi.org/10.1016/j.cbpa.2017.10.025.

(3) Ro, D.-K.; Paradise, E. M.; Ouellet, M.; Fisher, K. J.; Newman, K. L.; Ndungu, J. M.; Ho, K. A.; Eachus, R. A.; Ham, T. S.; Kirby, J.; Chang, M. C. Y.; Withers, S. T.; Shiba, Y.; Sarpong, R.; Keasling, J. D. Production of the Antimalarial Drug Precursor Artemisinic Acid in Engineered Yeast. *Nature* **2006**, *440* (7086), 940–943. https://doi.org/10.1038/nature04640.

(4) Nielsen, J.; Keasling, J. D. Engineering Cellular Metabolism. *Cell* **2016**, *164* (6), 1185–1197. https://doi.org/10.1016/j.cell.2016.02.004.

(5) Jiang, W.; Bikard, D.; Cox, D.; Zhang, F.; Marraffini, L. A. RNA-Guided Editing of Bacterial Genomes Using CRISPR-Cas Systems. *Nat. Biotechnol.* **2013**, *31*, 233.

(6) Jakočiūnas, T.; Bonde, I.; Herrgård, M.; Harrison, S. J.; Kristensen, M.; Pedersen, L. E.; Jensen, M. K.; Keasling, J. D. Multiplex Metabolic Pathway Engineering Using CRISPR/Cas9 in *Saccharomyces cerevisiae*. *Metab. Eng.* **2015**, *28*, 213–222. https://doi.org/10.1016/j.ymben.2015.01.008.

(7) Li, Y.; Lin, Z.; Huang, C.; Zhang, Y.; Wang, Z.; Tang, Y.; Chen, T.; Zhao, X. Metabolic Engineering of *Escherichia coli* Using CRISPR–Cas9 Meditated Genome Editing. *Metab. Eng.* **2015**, *31*, 13–21. https://doi.org/10.1016/j.ymben.2015.06.006.

(8) Roointan, A.; Morowvat, M. H. Road to the Future of Systems Biotechnology: CRISPR-Cas-Mediated Metabolic Engineering for Recombinant Protein Production. *Biotechnol. Genet. Eng. Rev.* **2016**, *32* (1–2), 74–91. https://doi.org/10.1080/02648725.2016.1270095.

(9) Bikard, D.; Jiang, W.; Samai, P.; Hochschild, A.; Zhang, F.; Marraffini, L. A. Programmable Repression and Activation of Bacterial Gene Expression Using an Engineered CRISPR-Cas System. *Nucleic Acids Res.* **2013**, *41* (15), 7429–7437. https://doi.org/10.1093/nar/gkt520.

(10) Depardieu, F.; Bikard, D. Gene Silencing with CRISPRi in Bacteria and Optimization of dCas9 Expression Levels. *Methods* **2020**, *172*, 61–75. https://doi.org/10.1016/j.ymeth.2019.07.024.

(11) Hogan, A. M.; Rahman, A. S. M. Z.; Lightly, T. J.; Cardona, S. T. A Broad-Host-Range CRISPRi Toolkit for Silencing Gene Expression in *Burkholderia*. *ACS Synth. Biol.* **2019**, *8* (10), 2372–2384. https://doi.org/10.1021/acssynbio.9b00232.

(12) Gilbert, L. A.; Horlbeck, M. A.; Adamson, B.; Villalta, J. E.; Chen, Y.; Whitehead, E. H.; Guimaraes, C.; Panning, B.; Ploegh, H. L.; Bassik, M. C.; Qi, L. S.; Kampmann, M.; Weissman, J. S. Genome-Scale CRISPR-Mediated Control of Gene Repression and Activation. *Cell* **2014**, *159* (3), 647–661. https://doi.org/10.1016/j.cell.2014.09.029.

(13) Gilbert, L. A.; Larson, M. H.; Morsut, L.; Liu, Z.; Brar, G. A.; Torres, S. E.; Stern-Ginossar, N.; Brandman, O.; Whitehead, E. H.; Doudna, J. A.; Lim, W. A.; Weissman, J. S.; Qi, L. S. CRISPR-Mediated Modular RNA-Guided Regulation

of Transcription in Eukaryotes. *Cell* **2013**, *154* (2), 442–451. https://doi.org/10.1016/j.cell.2013.06.044.

(14) Yeo, N. C.; Chavez, A.; Lance-Byrne, A.; Chan, Y.; Menn, D.; Milanova, D.; Kuo, C.-C.; Guo, X.; Sharma, S.; Tung, A.; Cecchi, R. J.; Tuttle, M.; Pradhan, S.; Lim, E. T.; Davidsohn, N.; Ebrahimkhani, M. R.; Collins, J. J.; Lewis, N. E.; Kiani, S.; Church, G. M. An Enhanced CRISPR Repressor for Targeted Mammalian Gene Regulation. *Nat. Methods* **2018**, *15* (8), 611–616. https://doi.org/10.1038/s41592-018-0048-5.

(15) Tanenbaum, M. E.; Gilbert, L. A.; Qi, L. S.; Weissman, J. S.; Vale, R. D. A Protein-Tagging System for Signal Amplification in Gene Expression and Fluorescence Imaging. *Cell* **2014**, *159* (3), 635–646. https://doi.org/10.1016/j.cell.2014.09.039.

(16) Perez-Pinera, P.; Kocak, D. D.; Vockley, C. M.; Adler, A. F.; Kabadi, A. M.; Polstein, L. R.; Thakore, P. I.; Glass, K. A.; Ousterout, D. G.; Leong, K. W.; Guilak, F.; Crawford, G. E.; Reddy, T. E.; Gersbach, C. A. RNA-Guided Gene Activation by CRISPR-Cas9–Based Transcription Factors. *Nat. Methods* **2013**, *10* (10), 973–976. https://doi.org/10.1038/nmeth.2600.

(17) Dominguez, A. A.; Lim, W. A.; Qi, L. S. Beyond Editing: Repurposing CRISPR–Cas9 for Precision Genome Regulation and Interrogation. *Nat. Rev. Mol. Cell Biol.* **2016**, *17* (1), 5–15. https://doi.org/10.1038/nrm.2015.2.

(18) Dove, S. L.; Hochschild, A. A Bacterial Two-Hybrid System Based on Transcription Activation. In *Protein-Protein Interactions*; Humana Press: New Jersey, 2004; Vol. 261, pp 231–246. https://doi.org/10.1385/1-59259-762-9:231.

(19) Dove, S. L.; Joung, J. K.; Hochschild, A. Activation of Prokaryotic Transcription through Arbitrary Protein–Protein Contacts. *Nature* **1997**, *386* (6625), 627–630. https://doi.org/10.1038/386627a0.

(20) Gregory, B. D.; Deighan, P.; Hochschild, A. An Artificial Activator That Contacts a Normally Occluded Surface of the RNA Polymerase Holoenzyme. *J. Mol. Biol.* **2005**, *353* (3), 497–506. https://doi.org/10.1016/j.jmb.2005.08.047.

(21) Ho, H.; Fang, J. R.; Cheung, J.; Wang, H. H. Programmable CRISPR-Cas Transcriptional Activation in Bacteria. *Mol. Syst. Biol.* **2020**, *16* (7). https://doi.org/10.15252/msb.20199427.

(22) Dong, C.; Fontana, J.; Patel, A.; Carothers, J. M.; Zalatan, J. G. Synthetic CRISPR-Cas Gene Activators for Transcriptional Reprogramming in Bacteria. *Nat. Commun.* **2018**, *9* (1). https://doi.org/10.1038/s41467-018-04901-6.

(23) Liu, Y.; Wan, X.; Wang, B. Engineered CRISPRa Enables Programmable Eukaryote-like Gene Activation in Bacteria. *Nat. Commun.* **2019**, *10* (1). https://doi.org/10.1038/s41467-019-11479-0.

(24) Yan, Q.; Xu, K.; Xing, J.; Zhang, T.; Wang, X.; Wei, Z.; Ren, C.; Liu, Z.; Shao, S.; Zhang, Z. Multiplex CRISPR/Cas9-Based Genome Engineering Enhanced by Drosha-Mediated SgRNA-ShRNA Structure. *Sci. Rep.* **2016**, *6* (1). https://doi.org/10.1038/srep38970.

(25) Haurwitz, R. E.; Jinek, M.; Wiedenheft, B.; Zhou, K.; Doudna, J. A. Sequence- and Structure-Specific RNA Processing by a CRISPR Endonuclease. *Science* **2010**, *329* (5997), 1355–1358. https://doi.org/10.1126/science.1192272.

(26) Nissim, L.; Perli, S. D.; Fridkin, A.; Perez-Pinera, P.; Lu, T. K. Multiplexed and Programmable Regulation of Gene Networks with an Integrated RNA and CRISPR/Cas Toolkit in Human Cells. *Mol. Cell* **2014**, *54* (4), 698–710. https://doi.org/10.1016/j.molcel.2014.04.022.

(27) Gao, Y.; Zhao, Y. Self-processing of Ribozyme-flanked RNAs into Guide RNAs *in Vitro* and *in Vivo* for CRISPR-mediated Genome Editing. *J. Integr. Plant Biol.* **2014**, *56* (4), 343–349. https://doi.org/10.1111/jipb.12152.

(28) Xie, K.; Minkenberg, B.; Yang, Y. Boosting CRISPR/Cas9 Multiplex Editing Capability with the Endogenous TRNA-Processing System. *Proc. Natl. Acad. Sci.* **2015**, *112* (11), 3570–3575. https://doi.org/10.1073/pnas.1420294112.

(29) Zetsche, B.; Heidenreich, M.; Mohanraju, P.; Fedorova, I.; Kneppers, J.; DeGennaro, E. M.; Winblad, N.; Choudhury, S. R.; Abudayyeh, O. O.; Gootenberg, J. S.; Wu, W. Y.; Scott, D. A.; Severinov, K.; van der Oost, J.; Zhang, F. Multiplex Gene Editing by CRISPR–Cpf1 Using a Single CrRNA Array. *Nat. Biotechnol.* **2016**, *35*, 31.

(30) Fonfara, I.; Richter, H.; Bratovič, M.; Le Rhun, A.; Charpentier, E. The CRISPR-Associated DNA-Cleaving Enzyme Cpf1 Also Processes Precursor CRISPR RNA. *Nature* **2016**, *532* (7600), 517–521. https://doi.org/10.1038/nature17945.

(31) Dong, D.; Ren, K.; Qiu, X.; Zheng, J.; Guo, M.; Guan, X.; Liu, H.; Li, N.; Zhang, B.; Yang, D.; Ma, C.; Wang, S.; Wu, D.; Ma, Y.; Fan, S.; Wang, J.; Gao, N.; Huang, Z. The Crystal Structure of Cpf1 in Complex with CRISPR RNA. *Nature* **2016**, *532* (7600), 522–526. https://doi.org/10.1038/nature17944.

(32) Zetsche, B.; Gootenberg, J. S.; Abudayyeh, O. O.; Slaymaker, I. M.; Makarova, K. S.; Essletzbichler, P.; Volz, S. E.; Joung, J.; van der Oost, J.; Regev, A.; Koonin, E. V.; Zhang, F. Cpf1 Is a Single RNA-Guided Endonuclease of a Class 2 CRISPR-Cas System. *Cell* **2015**, *163* (3), 759–771. https://doi.org/10.1016/j.cell.2015.09.038.

(33) Campa, C. C.; Weisbach, N. R.; Santinha, A. J.; Incarnato, D.; Platt, R. J. Multiplexed Genome Engineering by Cas12a and CRISPR Arrays Encoded on Single Transcripts. *Nat. Methods* **2019**, *16* (9), 887–893. https://doi.org/10.1038/s41592-019-0508-6.

(34) Kim, H. K.; Song, M.; Lee, J.; Menon, A. V.; Jung, S.; Kang, Y.-M.; Choi, J. W.; Woo, E.; Koh, H. C.; Nam, J.-W.; Kim, H. In Vivo High-Throughput Profiling of CRISPR–Cpf1 Activity. *Nat. Methods* **2017**, *14* (2), 153–159. https://doi.org/10.1038/nmeth.4104.

(35) Miao, C.; Zhao, H.; Qian, L.; Lou, C. Systematically Investigating the Key Features of the DNase Deactivated Cpf1 for Tunable Transcription Regulation in Prokaryotic Cells. *Synth. Syst. Biotechnol.* **2019**, *4* (1), 1–9. https://doi.org/10.1016/j.synbio.2018.11.002.

(36) Hu, J. H.; Miller, S. M.; Geurts, M. H.; Tang, W.; Chen, L.; Sun, N.; Zeina, C. M.; Gao, X.; Rees, H. A.; Lin, Z.; Liu, D. R. Evolved Cas9 Variants with Broad PAM Compatibility and High DNA Specificity. *Nature* **2018**, *556* (7699), 57–63. https://doi.org/10.1038/nature26155.

(37) Kleinstiver, B. P.; Sousa, A. A.; Walton, R. T.; Tak, Y. E.; Hsu, J. Y.; Clement, K.; Welch, M. M.; Horng, J. E.; Malagon-Lopez, J.; Scarfò, I.; Maus, M. V.; Pinello, L.; Aryee, M. J.; Joung, J. K. Engineered CRISPR–Cas12a Variants with Increased Activities and Improved Targeting Ranges for Gene, Epigenetic and Base Editing. *Nat. Biotechnol.* **2019**, *37* (3), 276–282. https://doi.org/10.1038/s41587-018-0011-0.

(38) Zhang, X.; Wang, J.; Cheng, Q.; Zheng, X.; Zhao, G.; Wang, J. Multiplex Gene Regulation by CRISPR-DdCpf1. *Cell Discov.* **2017**, *3* (1). https://doi.org/10.1038/celldisc.2017.18.

(39) Jeong, H.; Choi, S.-K.; Ryu, C.-M.; Park, S.-H. Chronicle of a Soil Bacterium: *Paenibacillus polymyxa* E681 as a Tiny Guardian of Plant and Human Health. *Front. Microbiol.* **2019**, *10*, 467. https://doi.org/10.3389/fmicb.2019.00467.

(40) Rütering, M.; Schmid, J.; Rühmann, B.; Schilling, M.; Sieber, V. Controlled Production of Polysaccharides–Exploiting Nutrient Supply for Levan and Heteropolysaccharide Formation in *Paenibacillus sp*. *Carbohydr. Polym.* **2016**, *148*, 326–334. https://doi.org/10.1016/j.carbpol.2016.04.074.

(41) Rütering, M.; Schmid, J.; Gansbiller, M.; Braun, A.; Kleinen, J.; Schilling, M.; Sieber, V. Rheological Characterization of the Exopolysaccharide Paenan in Surfactant Systems. *Carbohydr. Polym.* **2018**, *181*, 719–726. https://doi.org/10.1016/j.carbpol.2017.11.086.

(42) Rütering, M.; Cress, B. F.; Schilling, M.; Rühmann, B.; Koffas, M. A. G.; Sieber, V.; Schmid, J. Tailor-Made Exopolysaccharides—CRISPR-Cas9 Mediated Genome Editing in *Paenibacillus polymyxa*. *Synth. Biol.* **2017**, *2* (1). https://doi.org/10.1093/synbio/ysx007.

(43) Schmid, J. Recent Insights in Microbial Exopolysaccharide Biosynthesis and Engineering Strategies. *Curr. Opin. Biotechnol.* **2018**, *53*, 130–136. https://doi.org/10.1016/j.copbio.2018.01.005.

(44) Ji, X.-J.; Huang, H.; Ouyang, P.-K. Microbial 2,3-Butanediol Production: A State-of-the-Art Review. *Biotechnol. Adv.* **2011**, *29* (3), 351–364. https://doi.org/10.1016/j.biotechadv.2011.01.007.

(45) Schilling, C.; Ciccone, R.; Sieber, V.; Schmid, J. Engineering of the 2,3-Butanediol Pathway of *Paenibacillus polymyxa* DSM 365. *Metab. Eng.* **2020**, (in press).

(46) Gibson, D. G.; Young, L.; Chuang, R.-Y.; Venter, J. C.; Hutchison, C. A.; Smith, H. O. Enzymatic Assembly of DNA Molecules up to Several Hundred Kilobases. *Nat. Methods* **2009**, *6* (5), 343–345. https://doi.org/10.1038/nmeth.1318.

(47) Livak, K. J.; Schmittgen, T. D. Analysis of Relative Gene Expression Data Using Real-Time Quantitative PCR and the 2−ΔΔCT Method. *Methods* **2001**, *25* (4), 402–408. https://doi.org/10.1006/meth.2001.1262.

(48) Rühmann, B.; Schmid, J.; Sieber, V. Fast Carbohydrate Analysis via Liquid Chromatography Coupled with Ultra Violet and Electrospray Ionization Ion Trap Detection in 96-Well Format. *J. Chromatogr. A* **2014**, *1350*, 44–50. https://doi.org/10.1016/j.chroma.2014.05.014.

(49) Novotny, R.; Berger, H.; Schinko, T.; Messner, P.; Schäffer, C.; Strauss, J. A Temperature-Sensitive Expression System Based on the Geobacillus Stearothermophilus NRS 2004/3a SgsE Surface-Layer Gene Promoter. *Biotechnol. Appl. Biochem.* **2008**, *49* (1), 35. https://doi.org/10.1042/BA20070083.

(50) Niu, W.; Kim, Y.; Tau, G.; Heyduk, T.; Ebright, R. H. Transcription Activation at Class II CAP-Dependent Promoters: Two Interactions between CAP and RNA Polymerase. *Cell* **1996**, *87* (6), 1123–1134. https://doi.org/10.1016/S0092-8674(00)81806-1.

(51) Picossi, S.; Belitsky, B. R.; Sonenshein, A. L. Molecular Mechanism of the Regulation of Bacillus Subtilis GltAB Expression by GltC. *J. Mol. Biol.* **2007**, *365* (5), 1298–1313. https://doi.org/10.1016/j.jmb.2006.10.100.

(52) Dove, S. L.; Hochschild, A. Conversion of the Omega Subunit of *Escherichia coli* RNA Polymerase into a Transcriptional Activator or an Activation Target. *Genes Dev.* **1998**, *12* (5), 745–754. https://doi.org/10.1101/gad.12.5.745.

(53) Zafar, M. A.; Shah, I. M.; Wolf, R. E. Protein–Protein Interactions Between Σ70 Region 4 of RNA Polymerase and *Escherichia coli* SoxS, a Transcription Activator That Functions by the Prerecruitment Mechanism: Evidence for “Off-DNA” and “On-DNA” Interactions. *J. Mol. Biol.* **2010**, *401* (1), 13–32. https://doi.org/10.1016/j.jmb.2010.05.052.

(54) Shah, I. M.; Wolf, R. E. Novel Protein–Protein Interaction Between *Escherichia coli* SoxS and the DNA Binding Determinant of the RNA Polymerase α Subunit: SoxS Functions as a Co-Sigma Factor and Redeploys RNA Polymerase from UP-Element-Containing Promoters to SoxS-Dependent Promoters during Oxidative Stress. *J. Mol. Biol.* **2004**, *343* (3), 513–532. https://doi.org/10.1016/j.jmb.2004.08.057.

(55) Umarov, R. Kh.; Solovyev, V. V. Recognition of Prokaryotic and Eukaryotic Promoters Using Convolutional Deep Learning Neural Networks. *PLOS ONE* **2017**, *12* (2), e0171410. https://doi.org/10.1371/journal.pone.0171410.